Dimension effects of enclosures on ecological processes in pelagic systems

Gry Mine Berg,[1] *Patricia M. Glibert, and Chung-Chi Chen*[2]
Horn Point Laboratory, University of Maryland, Center for Environmental Science, Cambridge, Maryland 21613

Abstract

Several characteristics inherent to experimental ecosystems were examined for their influence on ecological processes in five cylindrical indoor benthic–pelagic enclosures of different size and shape. Ecosystem development diverged significantly among the mesocosm dimensions even though environmental parameters such as surface photosynthetically available radiation (400–700 nm), turbulence intensity, water exchange rate, and nutrient input were held constant across systems. Here we show that factors that lead to the development of different plankton assemblages can be related to mesocosm geometry. The ratio of light-receiving surface area-to-water column volume $(A_s : V)$ was shown to control both the rate of NO_3^- consumption and gross primary productivity. The attenuation of water column irradiance was positively correlated with the wall area-to-volume ratio $(A_w : V)$. This was manifested in greater light attenuation in systems with a high $A_w : V$ ratio. In addition, notably greater microalgal biomass developed on the walls in systems with a high $A_w : V$ ratio. Finally, the total surface area-to-volume ratio $(A_t : V)$ of the mesocosms influenced the rate of energy gain and dissipation and water column temperature. The differences in temperature among dimensions possibly affected biological parameters such as bacterial biomass. Although the influence of area-to-volume effects on biological components in artificial systems may be substantial, our analysis indicates that some of these effects may be predictable and that future experiments can be explicitly designed to minimize artifacts of enclosure.

Experimental ecosystems (mesocosms) are often used to examine ecological interactions and they allow investigators to observe one discrete body of water for a sufficient length of time to characterize nutrient fluxes and trophic interactions (Lalli 1990; Oviatt 1994; Glibert 1998). Mesocosms are particularly useful in studies of energy and material transfer from one trophic level to another, in studies of interactions between plankton and benthic communities, and in studies of chemical or biogeochemical transformations of nutrients or pollutants (cf. Takahashi et al. 1975; Parsons et al. 1978; Elmgren et al. 1980; Grassle and Grassle 1984; Oviatt et al. 1987; Doering et al. 1989; Egge and Aksnes 1992; Heiskanen et al. 1996).

Nevertheless, it is well recognized that artifacts and constraints of experimental enclosures pose limitations on how readily results can be extrapolated from artificial to natural systems (Pilson and Nixon 1980; Brockmann 1990; Oviatt 1994). Experimental systems are inherently limited in their ability to reproduce nature accurately through omission of higher trophic levels or water column structure (Carpenter 1996). In addition, ecosystem couplings can be influenced by two types of enclosure effects, fundamental scaling effects and artifacts of enclosure (Petersen et al. 1997). Fundamental scaling effects can be attributed to characteristics such as depth that are common to all ecosystems, whereas artifacts of enclosure are characteristics of experimental systems that differ from natural ecosystems (Petersen et al. 1997).

A commonly used criterion for the design of mesocosm systems is that some variables, e.g., the sediment area-to-volume ratio or water exchange rate, should be similar to the natural system to which data will be applied (i.e., Nixon et al. 1980; Oviatt et al. 1987). However, regardless of scaling similarities between enclosed systems and their natural counterparts, biological parameters in enclosures very often behave differently than the same parameters in natural systems (French and Watts 1989; Oviatt et al. 1980, 1989; Axler and Reuter 1996). In enclosures of differing physical scales, food web dynamics may be affected to varying degrees, creating trophic interactions that differ with dimension and differ from those of a natural system (Kuiper et al. 1983; Stephenson et al. 1984). A characteristic artifact that can produce such imbalances includes the large wall area-to-volume ratio of many enclosures; the growth of material on walls has been shown frequently to dominate rate processes of the pelagic phytoplankton (Kroer and Coffin 1992; Oviatt 1994; Chen et al. 1997). In an effort to understand whether results from experimental systems of very different physical proportions can be compared when treatments are similar, a study was undertaken to quantify variability in biological parameters resulting from differences in physical scale and associated enclosure artifacts. Environmental variables such as room temperature, photosynthetically available radiation (PAR), and turbulence intensity were held constant, whereas physical dimensions such as radius and depth of the enclo-
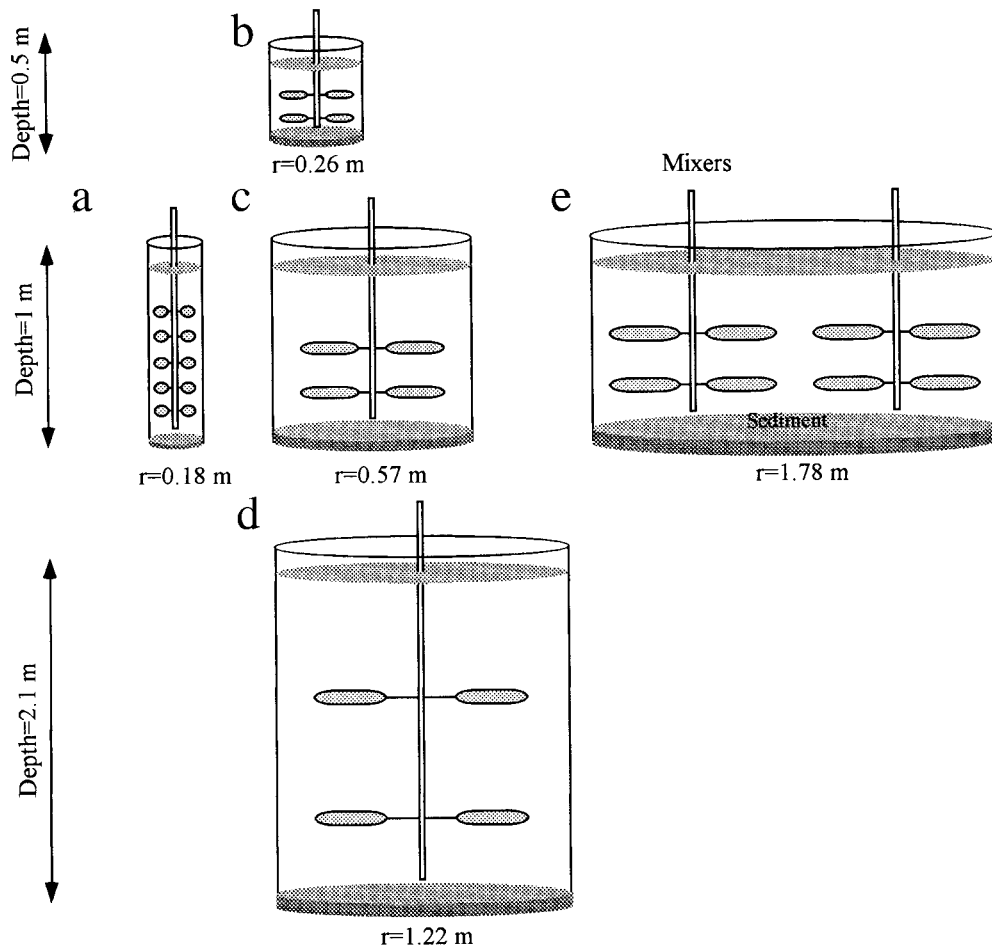
Berg et al.

Fig. 1.   Mesocosm schematic (drawn to scale). Constant depth series (a, c, e) depicted horizontally and constant shape series (b, c, d) depicted vertically.

sures were varied. In the present analysis, we examined the influence of horizontal surface area-to-volume ratio ($A_s : V$), wall area-to-volume ratio ($A_w : V$), total surface area-to-volume ratio ($A_t : V$), and artificial lighting of five different dimension enclosures on nitrogen consumption, bacterial predominance, wall, and water column chlorophyll biomass.

Materials and methods

Enclosure design—A 4-week experiment was conducted in the spring of 1994 at an indoor mesocosm facility located at Horn Point Laboratory, University of Maryland. Cylindrical enclosures of five distinct combinations of depth and diameter, each with three replicates, were used (Fig. 1). The enclosures were identified as dimensions A, B, C, D, and E in order of increasing diameter (Table 1). They were organized into two series: the constant depth series was designed to examine radius effects, and the constant shape series was designed to examine the combined effects of radius and depth. The enclosures in the constant depth series (dimensions A, C, and E) were of identical water column depth (1 m), whereas the constant shape series (B, C, and D) had a constant ratio of radius : depth (Fig. 1). The C dimension was

common to both series. The mesocosm $A_w : V$ ratio was inversely related to the radius of the mesocosms and increased in the order of E, D, C, B, and A (Table 1). All systems were constructed of Sun-Lite®, a white fiberglass-reinforced glazing material (Kalwall Inc.). Illumination was provided by cool-white fluorescent lights and incandescent bulbs on a 12 : 12 light : dark cycle. The mean PAR was 277 μE m^{-2} s^{-1}, and the range in PAR was 246–314 μE m^{-2} s^{-1} (Table 1). Mixing was provided by paddles attached to a polyvinyl chloride rod rotating 4 h on and 2 h off during the entire time course. Rotation rates were selected to simulate the turbulence intensities associated with a semidiurnal tidal cycle in Chesapeake Bay (Sanford 1997). The root-mean-square turbulent velocity, u_{RMS}, a proxy for turbulence intensity, was conserved across dimensions based on enclosure mixing configurations (Table 1; Sanford 1997). This mixing regime resulted in minimal resuspension of bottom sediments, and turbidity due to nonphotosynthetic particles was therefore low throughout the experiment (Petersen et al. 1997).

Sediment composition and water exchange—To each mesocosm, 10 cm of sediment was added in the form of a mixture of commercial sand and sediment from the Chop-

Table 1. Physical parameters of mesocosms.

Physical parameter	Mesocosm				
	A	B	C	D	E
Volume (m³)	0.10	0.10	1.00	10.0	10.0
Depth (m)	1.0	0.5	1.0	2.1	1.0
Radius : depth	0.18	0.56	0.56	0.56	1.78
Top surface area : volume (m⁻¹)	1.0	2.1	1.00	0.46	1.0
Wall area : volume (m⁻¹)	11.3	7.51	3.60	1.64	1.12
Total surface area : volume (m⁻¹)	13.3	11.7	5.6	2.6	3.1
Mixing time (min)	4	4	12	39	15
Turbulence intensity (cm s⁻¹)	2	2	2	2	2
Surface PAR (μE m⁻² s⁻¹)	246	291	314	248	288
*Light attenuation coefficient, K_d (m⁻¹)	1.43	1.36	1.09	0.73	0.82

* Mean coefficient of diffuse downwelling attenuation of PAR measured during the time course.

tank River, a subestuary of Chesapeake Bay. Prior to the experiment, the sediment mixture was collected in a common tank, allowed to go anaerobic to reduce the abundance of benthic infauna, and homogenized by mixing with shovels. After mixing, the sediment slurry contained 1% organic matter. The mesocosms were filled incrementally with sediments and water to minimize heterogeneity among systems. The systems were left to equilibrate for several days before the start of the experiment. Next, the mesocosms were drained and filled with Choptank River water (salinity 8‰). Larvae, polychaete worms, and small crustacea were included in the initial fill water, while fish and other predators were excluded. Over time, amphipods and barnacles became the dominant predators in these systems. After a period of 24 h, the lights and mixers were turned on in the tanks and sampling began after 72 h. For the remainder of the experiment, 10% of the water volume in each tank was exchanged daily with <2-μm filtered Choptank River water.

Biological parameters—During the time course, all 15 mesocosms were sampled twice weekly for nutrient concentrations, chlorophyll *a* (Chl *a*), particulate carbon and nitrogen (PC and PN), and bacterial abundance. Dissolved nutrients (NH_4^+, NO_3^-, and Si[OH]$_4$) were analyzed immediately following filtration through precombusted GF/F filters, on a Technicon AAII autoanalyzer using standard methods (Zimmerman et al. 1977; Whitledge et al. 1981). Chl *a* was determined with a Turner Designs fluorometer on samples stored frozen at −20°C until extraction in 90% acetone. Samples for PC and PN were collected on 25-mm precombusted GF/F filters (450°C for 2 h) under low vacuum (<100 mm Hg) and stored frozen (−20°C) until dried and analyzed on a Control Equipment CHN analyzer (within 2–3 weeks). Heterotrophic bacteria, preserved in glutaraldehyde (1% final concentration), were enumerated by acridine orange direct counts (Hobbie et al. 1977) using a Zeiss Axiophot epifluorescence microscope equipped with a blue exciter filter. Bacterial carbon biomass was estimated by multiplying bacterial abundance by a factor of 20 fg C cell⁻¹ (Lee and Fuhrman 1987). Microalgal wall growth was determined by measuring Chl *a* concentration on vertical strips made of the same fiberglass material as the walls themselves, attached to the walls of the mesocosms. The strips were put up at the

beginning of the experiment and taken down the day after the experiment ended. The attached biomass was scraped off with a razor, and Chl *a* concentrations were measured using the same method as with water column Chl *a* (Chen et al. 1997). Rates of gross primary productivity (GPP) were determined for 17 points during the 4-week time course by measuring dawn–dusk–dawn changes in O_2 using polarographic electrodes (Petersen et al. 1997).

Environmental parameters—Irradiance measurements were made using two separate approaches. Daily measurements of the photon flux density of PAR (the number of photons in the 400–700-nm waveband incident per unit time on a unit surface) were taken vertically along several points in each mesocosm using a LiCor SPA-QUANTUM hemispherical 2π sensor connected to a LiCor LI-1000 data logger. The diffuse downwelling attenuation coefficient, K_d (m⁻¹), was calculated for each mesocosm from the slope of the linear regression of log-transformed changes in PAR with depth. Surface PAR did not give an accurate measure of total incident irradiance, as much of the incandescent light energy was not accounted for in the 400–700-nm range. Thus, in addition to PAR measurements, total incident irradiance in the 200–50,000-nm range was measured with a thermopile light sensor (Eppley Laboratory).

Temperature measurements were logged continuously on a diel cycle in each mesocosm with in situ thermisters throughout the time course.

Statistical analyses—All statistical analyses were made using Statistical Analysis Systems (SAS) software (SAS Institute). The effect of mesocosm type on nutrient consumption and biomass accumulation over time was investigated using repeated-measures analysis (Crowder and Hand 1990). The effect of mesocosm type on light attenuation and microalgal wall growth was examined using analysis of variance (ANOVA). Means were compared using the least significant difference approach. Measures of variance were reported as ±1 standard error (SE).

Results

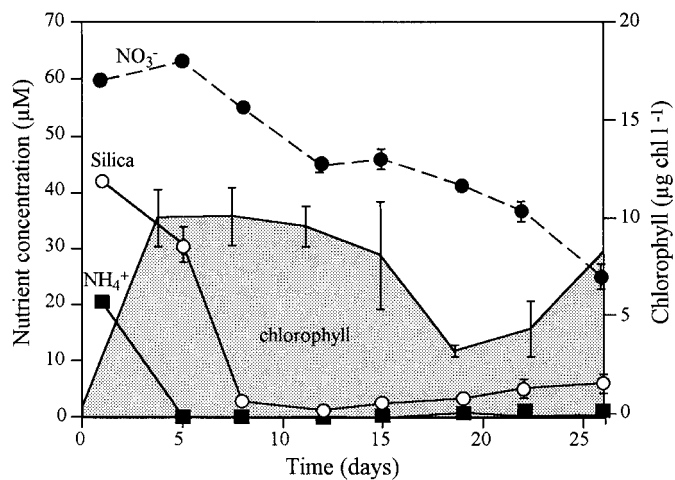*General trends in nutrient and chlorophyll concentrations*—Throughout the experiment, nutrient concentrations

Fig. 2. Representative time course of changes in NH_4^+, NO_3^-, $Si(OH)_4$, and Chl *a* concentrations from dimension C. Error bars represent ±1 standard deviation of three replicate mesocosms.

in the 10% daily exchange water remained fairly consistent. Median concentrations of nutrients in the fill water were 64 μM NO_3^-; 0.4 μM NH_4^+; and 31 μM $Si(OH)_4$. During the first 5 d of growth, NH_4^+ and $Si(OH)_4$ declined rapidly in all the mesocosms, concurrent with the initial bloom of phytoplankton (Fig. 2). During the same period, concentrations of NO_3^- decreased by varying amounts depending on mesocosm dimension. As with rates of nutrient depletion, the timing of the peaks in chlorophyll biomass varied among dimensions (data not shown). Consequently, nutrient and Chl *a* concentrations differed significantly among dimensions as examined using repeated-measures analysis (Table 2).

Nutrient dynamics and gross primary productivity—Net water column NO_3^- depletion (difference in nutrient concentration between days 1 and 26) and mean GPP, a measure of net primary productivity and respiration, were significantly correlated across dimension (Table 3). Net NO_3^- depletion was greatest in dimension B (60 μM) followed by dimension E (42 μM), corresponding with peaks in GPP of 6.5 and 4 mg O_2 liter^{-1} d^{-1} in B and E, respectively (Fig. 3a). There was a 5.2-fold range in GPP among the dimensions in the constant shape series (B–D), while the range in mean GPP among the dimensions in the constant depth series (A–E) was 1.4-fold. Although differences within the constant depth series were small, there were significant differences between dimensions A and E in both net NO_3^- depletion and GPP. Dimension C fell in between and was not significantly different from either A or E.

In the present and several subsequent mesocosm experiments, sediment–water nutrient fluxes were found to be minimal. During this experiment, net fluxes of the major nutrients NH_4^+ and PO_4^{3-} were into the sediments in all dimensions, while NO_3^- was the only nutrient with a net flux (15 μM m^{-2} h^{-1}) into the water column (Cornwell et al. unpubl. data). Direct rates of NO_3^- uptake in the water column were greatest in dimensions E and C (rates of ^{15}N uptake to be reported elsewhere). In comparison, the rate of NO_3^- uptake was 50% less in dimension B, while net NO_3^-

Table 2. Probability values calculated for testing effects of treatment (differences among mesocosm dimensions), time, and treatment × time interaction ($n = 120$) on silica, NH_4^+, NO_3^-, and Chl *a* using repeated-measured analysis.

Source of variation	Silica	NH_4^+	NO_3^-	Chl *a*
Treatment	0.0085	0.0003	0.0001	0.0045
Time	0.0001	0.0001	0.0001	0.001
Treatment × time	0.0001	0.0001	0.0001	0.0557

depletion was 32–40% greater than in dimensions E and C (Table 4).

Changes in chlorophyll biomass and light intensity—Chl *a* concentrations peaked in dimensions E and B, 19.4 and 17.4 μg Chl liter^{-1}, respectively. These concentrations were significantly higher than the peak concentration in dimension D (Fig. 3b). Mean Chl *a* concentrations were greatest in the constant depth series (range 6.67–7.99 μg Chl liter^{-1}). In this series, mean Chl *a* did not differ significantly among dimensions (Fig. 3b). Mean Chl *a* differed significantly between the constant depth series and dimension D.

Microalgal biomass on the walls was normalized per unit mesocosm water volume according to Chen et al. (1997), where the biomass expressed per m^2 wall area was multiplied by the total wall area (m^2) and divided by volume (m^3) of the respective dimensions to give microalgal Chl *a* per unit water column volume (mg m^{-3} or μg liter^{-1}). By the end of the time course, dimension D had the highest concentration of wall microalgal biomass (56 ± 30 μg Chl liter^{-1}), followed by dimensions A and B (Fig. 3c). In dimensions C and E where water column Chl *a* biomass was more comparable to wall microalgal biomass, wall Chl *a* peaked at 18 and 11 μg Chl liter^{-1} and water column Chl *a* averaged concentrations of 7 and 8.5 μg Chl liter^{-1}, respectively (Fig. 3b,c). With the exception of dimension D, there was a significant relationship between Chl *a* and the A_w:V ratio of the mesocosms (Table 3).

Heterotrophic influence—Compared with differences in absolute mean bacterial abundance (~30% among dimensions), the fraction of the total particulate material (measured by CHN analysis) composed of bacteria was estimated to be a more accurate indicator of bacterial influence among di-

Table 3. Linear regressions between bacterial carbon fraction versus total incident light energy (W m^{-2}); diel temperature range (°C) versus total incident light energy; wall microalgal biomass (μg Chl liter^{-1}) excluding dimension D versus A_w:V ratio (m^{-1}); and mean gross primary productivity, GPP (mg O_2 liter^{-1} d^{-1}), versus net NO_3^- depletion (μM).

Regression variables	Slope	r^2
Bacterial fraction versus total light	0.00075	0.89*
Diel temperature versus total light	0.022	0.81*
Wall microalgae versus A_w:V	3.17	0.99†
GPP versus net NO_3^- depletion	0.108	0.98†

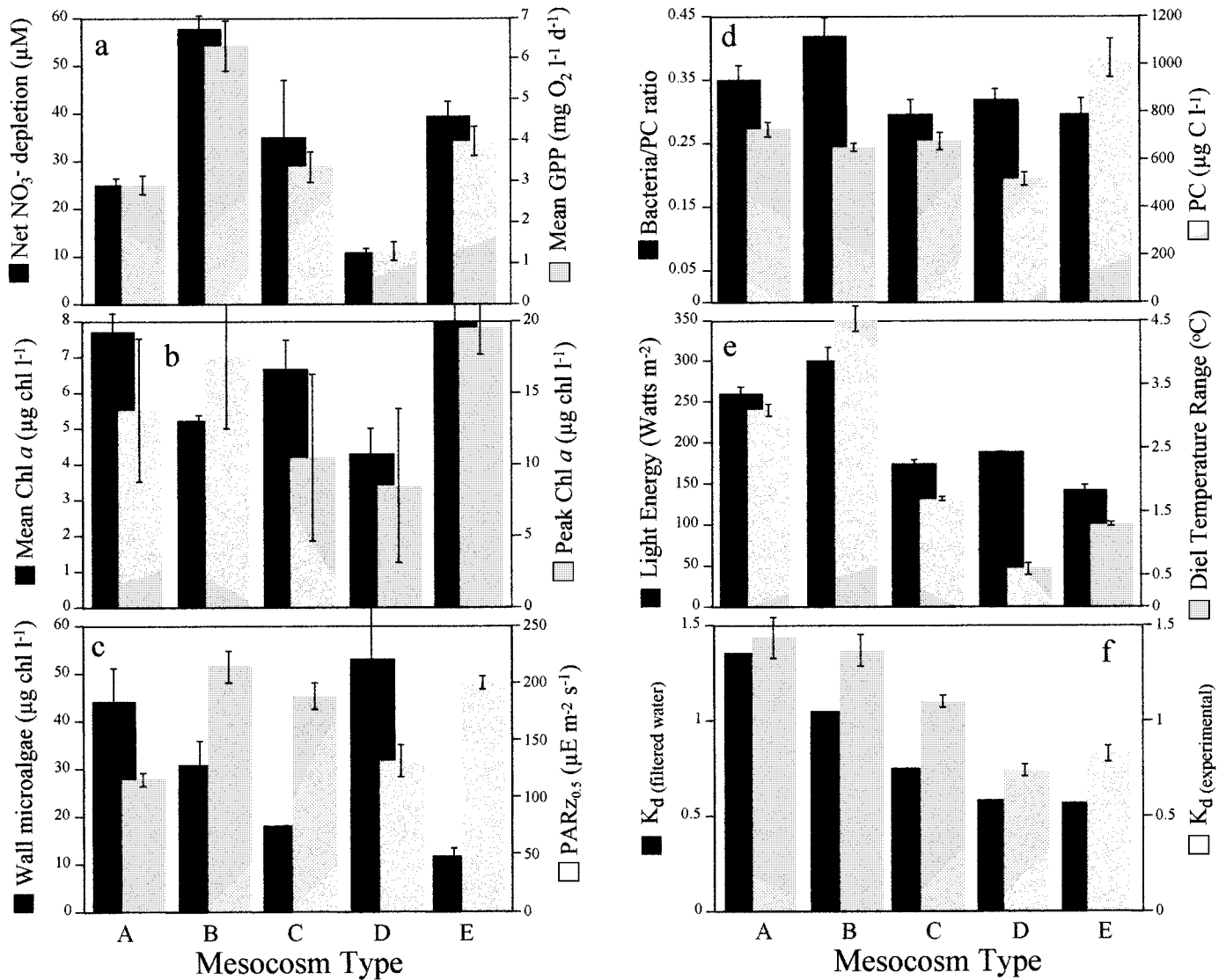* Significant correlation at $P<0.05$.
† Significant correlation at $P<0.01$.

Fig. 3. (a) Net NO_3^- depletion (μM) and mean GPP (mg O_2 liter^{-1} d^{-1}) versus mesocosm dimension. (b) Mean Chl *a* and peak Chl *a* concentrations (μg Chl liter^{-1}) versus mesocosm dimension. (c) Microalgal biomass on the walls (μg Chl liter^{-1}) versus mesocosm dimension. (d) Fraction of bacterial carbon : total particulate carbon versus mesocosm dimension. (e) Total incident light energy (W m^{-2}) and diel temperature range (°C) versus mesocosm dimension. (f) Mean light attenuation coefficient, K_d, obtained during the time course and in filtered water versus mesocosm dimension. Error bars in all six panels represent ±1 standard deviation of three replicate mesocosms.

Table 4. Range in time averaged rates of NO_3^- uptake (ρ) and net NO_3^- depletion (ΔNO_3^-) ± standard error of three replicate mesocosms.

Dimension	*ρ (μM NO_3^- h^{-1})	ΔNO_3^- (μM)
A	0.149 ± 0.005	24.77 ± 0.97
B	0.092 ± 0.011	57.35 ± 1.33
C	0.187 ± 0.006	34.87 ± 2.63
D	0.154 ± 0.018	10.57 ± 0.67
E	0.187 ± 0.016	39.37 ± 1.33

* A trace amount of NO_3^- was added to a 500-ml sample that was incubated for 1 h in a polycarbonate bottle. Incubations were terminated by filtration through GF/F filters. Filters were prepared and analyzed by mass spectrometry according to Glibert et al. (1991). Uptake rates were calculated according to Glibert and Capone (1993).

mensions. Total particulate carbon varied around 600 μg C liter^{-1} in all dimensions except in dimension E where the mean concentration was 1,000 μg C liter^{-1} (Fig. 3d). Bacterial carbon biomass (estimated from bacterial abundance) as a fraction of the total particulate carbon was 35% greater in dimension B compared to dimensions C and E (Fig. 3d). The variability in bacterial carbon biomass normalized to total particulate carbon among mesocosm dimensions correlated well with variability in total incident light energy (Table 3).

Irradiance and temperature variability—In these systems, total incident light energy showed a greater than twofold range among the different mesocosm types. Dimensions A and B received the most total light energy, up to 300 W m^{-2},

while C, D, and E received the least (Fig. 3e). Similar to the trend in total incident light energy, mean daily water temperature showed a decreasing trend in the order B > A + C > D + E (data not shown). An eightfold difference in the diel water column temperature range resulted from differing rates of energy gain and dissipation depending on mesocosm dimension. The diel temperature range was maximal in dimension B (4.5°C) and minimal in dimension D (0.56°C) (Fig. 3e). Greater than 80% of the variability in the temperature range among the systems was explained by differences in total incident energy (Table 3).

Water column light field (Fig. 3c), denoted by PAR at mid-depth ($PARz_{0.5}$), was not correlated significantly with either mean or peak water column Chl *a* concentrations or with wall microalgal Chl *a* ($P > 0.5$). The attenuation of PAR with water column depth related positively to mesocosm dimension, denoted by the $A_w : V$ ratio (Table 3). Light attenuation coefficients, K_d (m^{-1}), calculated for each dimension from measurements of PAR made when the mesocosms were filled with filtered water, were similar to those calculated from PAR measured during the experiment (Fig. 3f).

Discussion

It has long been recognized that a chief concern with mesocosm studies is the large ratio of $A_w : V$ and the artifacts that this poses in terms of wall growth in close contact with the water column (cf. McAllister et al. 1961). One way to avoid this problem is to implement whole-ecosystem studies in lakes or oceans (cf. Carpenter et al. 1995). However, unlike limnological ecosystem studies, whole ecosystem-scale fertilization experiments to study interactions in marine ecosystems are not readily feasible for both financial and environmental reasons. While the iron fertilization experiments in the equatorial Pacific have proven a notable exception to this rule (Coale et al. 1996), large-scale fertilization experiments cannot be safely employed to study nearshore ecosystem interactions. As coastal systems are being affected increasingly by land-based nutrient inputs, marine mesocosms are emerging as a powerful tool to study these effects on coastal plankton communities.

In the present study, results from estuarine mesocosms of different physical proportions were compared to quantify variability in plankton dynamics. In addition, biological and environmental parameters in the mesocosms were compared with parameters in a natural estuarine system. Higher trophic levels such as gelatinous zooplankton and fish were excluded from the study. Ecosystem differences were manifested by differences in chlorophyll biomass, wall growth, gross primary productivity, bacterial carbon biomass as a fraction of total particulate biomass, and rates of nutrient utilization. The differences in these biological parameters with system shape and size scaled not only with the wall area-to-volume ratio but also with the horizontal surface area-to-volume ratio and with the total surface area-to-volume ratio.

Surface area-to-volume ratio—Gross primary productivity was closely coupled with NO_3^- depletion, indicating that the processes consuming NO_3^-, whether they occurred in the water column or on the walls, were dominant in terms of driving GPP in the mesocosms. Both mean GPP and net NO_3^- depletion scaled linearly with the $A_s : V$ ratio of the systems (Fig. 4a) that controlled the average light field, $PARz_{0.5}$. Thus, dimensions with the larger $A_s : V$ ratio were more productive (i.e., B) than dimensions with a smaller $A_s : V$ ratio (i.e., D). Within the constant depth series, GPP increased proportional to $PARz_{0.5}$ in the order A, C, E.

In addition to differences in the water column light field, differences in the relative biomass of grazers among dimensions may also have influenced productivity. Dimension B, which experienced the greatest overall rates of GPP and low Chl *a* concentrations, evidenced 2.5–4-fold greater copepod biomass (μg C liter^{-1}) compared with the other dimensions (Roman et al. unpubl. data). The pattern in dimension B was consistent with that observed in natural communities where high rates of primary productivity result from zooplankton grazing and other losses due to sinking and physical exchange that continually reduce phytoplankton standing stocks (Banse 1992; Landry et al. 1997).

The interactions between light intensity, productivity, and grazing observed among the dimensions appeared to reflect interactions observed in coastal plankton communities. Dimension B developed in a manner similar to a typical summer community dominated by picoplankton and high rates of grazing and productivity (cf. Glibert et al. 1991; Bode and Dortch 1996). In contrast, dimensions A, C, and E developed in a manner similar to a spring community where the high biomass of diatoms may result in a lower water column light intensity and lower rates of productivity compared to a typical summer community (Glibert et al. 1995; Malone et al. 1996).

Wall area-to-volume ratio—Mesocosm geometry figured substantially in the vertical attenuation of light (Fig. 4b). This contrasts with a natural system where the majority of light is typically partitioned among phytoplankton, dissolved constituents, and water (Kirk 1994). Part of the close correlation between light attenuation and mesocosm shape could be explained by the decrease with depth in the solid angle, ω (the angle through which the flux of downwelling irradiance is detected). The rate of the decrease in ω was dependent on enclosure design and was a function of the distance of the overhead lighting and enclosure radius (Fig. 5). Similar to the relative differences in K_d, the decrease in ω was inversely proportional to enclosure radius (Fig. 5b).

The range of mesocosm K_d (0.7–1.44 m^{-1}) was within the range observed in Chesapeake Bay (K_d ranging between 0.6 and 1.6 m^{-1} in spring and 0.4 and 0.9 m^{-1} in summer; Glibert et al. unpubl. data), but the relationship between K_d and mesocosm water column light field was not intuitive. For example, dimension B had a larger K_d compared with dimension D, but the net effect of a greater water column depth in the latter dimension was a lower $PARz_{0.5}$ than in the former dimension. $PARz_{0.5}$ was lower in the narrow, deeper dimensions (A and D) compared with the wide, shallow dimensions (B and E). In the narrow dimensions, there was no significant relationship between Chl *a* and K_d ($r^2 < 0.008$, $P > 0.8$), suggesting that vertical attenuation of PAR was minimally influenced by phytoplankton biomass. Con-
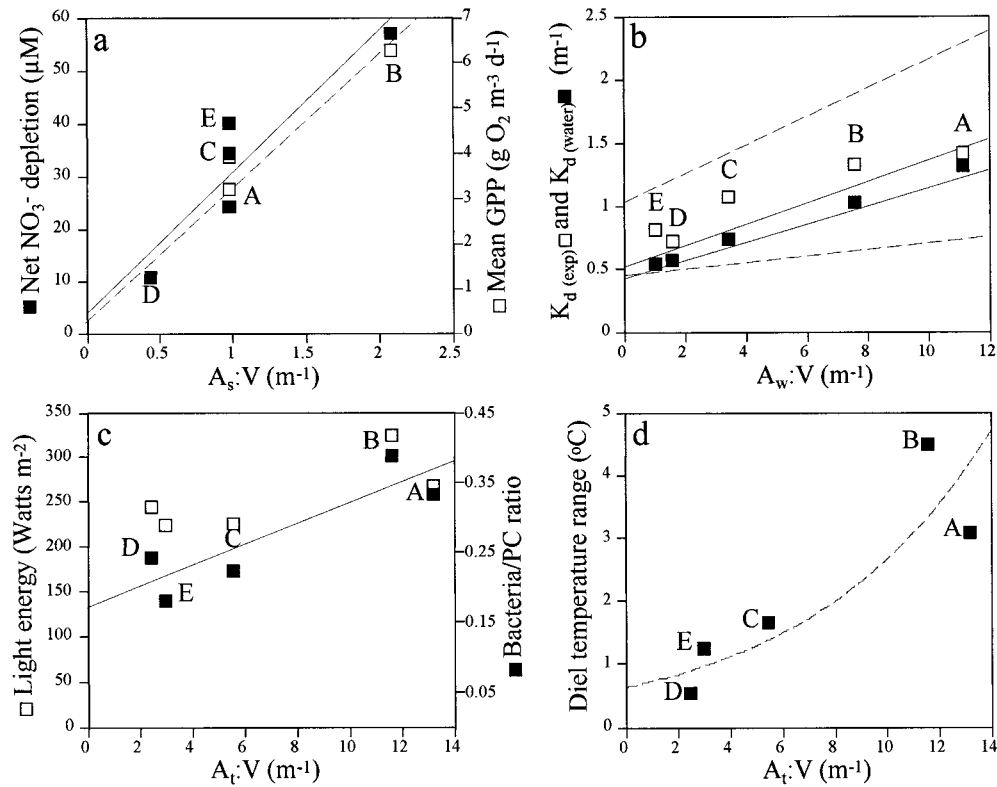
Fig. 4. (a) Net change in NO_3^- and mean GPP as a function of mesocosm A_s:V ratio. Dashed line: mean GPP = 2.96(A_s:V) + 0.244, r^2 = 0.94, P < 0.01; solid line: D_{NO3-} = 26.88(A_s:V) + 3.496, r^2 = 0.86, P < 0.05. (b) Mean light attenuation coefficient, K_d, in filtered water (dark square) r^2 = 0.99, slope = 0.077, intercept = 0.465, P < 0.01; and during the time course (open square) (n = 10) r^2 = 0.89, slope = 0.068, intercept = 0.743, P < 0.05; as a function of mesocosm A_w:V ratio. Solid line indicates confidence interval for K_d in filtered water, and broken line indicates confidence interval for K_d during the time course. (c) Change in light energy (LE) and in the bacteria:particulate carbon fraction as a function of mesocosm A_t:V ratio: LE = 11.66A_t:V + 128.8, r^2 = 0.8, P < 0.05. (d) Exponential increase (R_t = 0.61$e^{[0.1453At:V]}$) in diel temperature range (R_t) with mesocosm A_t:V ratio.

versely, in dimensions B and E, K_d varied significantly with changes in Chl *a* (P < 0.02), implying that a portion of the variability in K_d was attributable to phytoplankton rather than mesocosm geometry.

Growth of microalgae on the walls of the mesocosms (Fig. 3c) also influened light attenuation. However, compared to the effect of wall flora on pelagic processes (cf. Chen et al. 1997), the effect of wall flora on K_d was too small to be observed in our data. The influence of wall growth on nitrogen depletion and GPP was particularly evident in dimension D. Here, biomass accumulation at the wall exceeded that predicted based on mesocosm A_w:V ratio, and wall GPP exceeded water column GPP (Chen et al. 1997). In this dimension, phytoplankton NO_3^- uptake was consistent with rates in the other dimensions, yet net NO_3^- depletion over the course of the experiment was minimal. This was unexpected based on the amount of wall flora present, suggesting a source of NO_3^- to the system. This source could partly be explained by nitrogen mineralization processes in the sediments. Due to the depth of the water column, dimension D had the lowest light intensity at the sediment surface (~20% I_o). Based on the observed flux of NO_3^- out of the sediments

and nitrogen mass balance calculations, we infer that nitrification may have contributed substantially to the total NO_3^- input, fuelling a dramatic increase in wall growth. The pattern of increased microalgal wall growth in dimension D was repeated in subsequent experiments (Chen et al. 1997).

Total surface area-to-volume ratio—In the present study, there was a lack of correlation between bacterial abundance and size of the system, primary producer biomass, or grazers (P > 0.05). When bacterial abundance was normalized to carbon biomass in the phytoplankton size range, the majority of variability in the bacterial fraction was attributable to differences in total light energy among mesocosm dimensions (Table 3; Fig. 3d,e).

We suggest that the close coupling between total incident light energy (W m^{-2}) and bacterial predominance was related to the heat emitted from the incandescent lights used during this study. Incandescent lighting from tungsten bulbs is hotter and emits more energy in the infrared than cool-white fluorescent lights. The combination of cool-white fluorescent and incandescent bulbs probably produced a gradient of light biased toward the red with a high rate of absorption by water
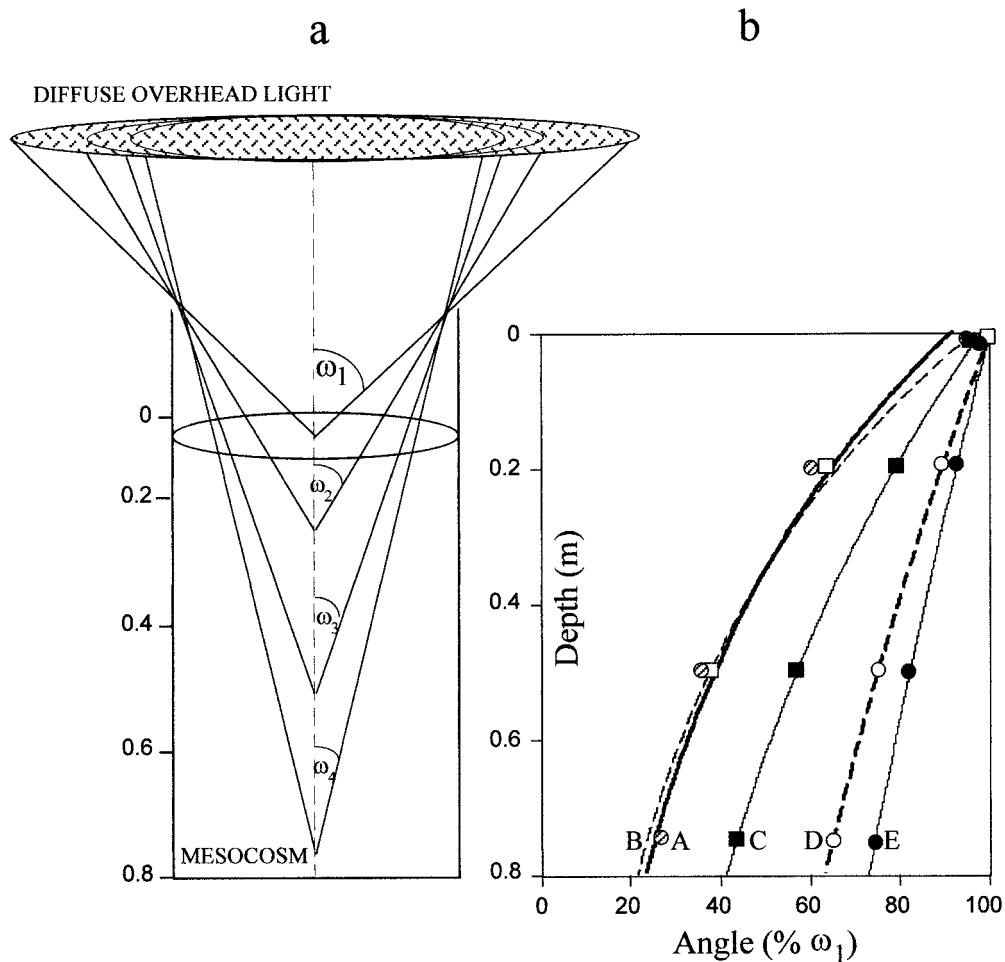
Fig. 5. (a) Illustration of the change with depth in angle, ω, through which the downwelling irradiance from the overhead light banks is detected in a mesocosm. (b) Decrease in ω with depth as a function of dimension.

of the energy greater than 600 nm (cf. Nelson and Prézelin 1990; Kirk 1994). Greater incident total light energy resulted in a proportionally greater input of longer wavelength light, some of which likely contributed to heating up the water surface. The heating effect was most evident in the systems with a large A_t : V ratio (dimensions A and B) where the water warmed up more rapidly during the day when lights were on and cooled more rapidly at night when the lights were turned off (Fig. 4c,d).

The uncoupling of bacterial abundance with resource parameters observed in the present study contrasted with dynamics in several other enclosure studies (cf. Bjørnsen et al. 1988; Painting et al. 1989; Riemann et al. 1990) and in the natural environment. Over shorter time scales, bacterial abundance and production typically track phytoplankton productivity, abundance, or both (Lancelot and Billen 1984; Malone et al. 1986; Bratbak et al. 1990; Simon et al. 1992); this relationship is thought to be driven by the release of dissolved organic carbon (Derenbach and Williams 1974; Cole et al. 1982). In the enclosures, bacterial abundance and autotrophic biomass were coupled in a subsequent time

course where the incandescent bulbs were removed and only cool-white fluorescent bulbs were used.

Summary—A distinct advantage with ecosystem studies in experimental enclosures is that they allow investigators to study the development of the same assemblage over time. In enclosures of different dimensions, ecosystem development may diverge although initial conditions are the same. In the present study, pelagic processes within dimension E appeared to be least affected by enclosure effects and compared most easily to a natural analog such as Chesapeake Bay. This dimension demonstrated the highest amount of productivity per unit A_s : V; hence, it was the only system in which the pelagic community was not dominated by rate processes occurring at the walls. A likely contributing factor was the enhanced light availability and primary producer biomass compared to the other dimensions. In addition to light availability, productivity, Chl a concentration, and bacterial/total particulate carbon fraction in this dimension compared well with Chesapeake Bay (Table 5). As presented here, our results imply that trophic interactions between en-

Table 5. Comparison of biological parameters in dimension E to the midstation of Chesapeake Bay.

| | Dimension E | Chesapeake Bay | | Source |
		Spring	Summer	
Productivity (mg O_2 liter^{-1} d^{-1})	4	5	7–8	Smith and Kemp 1995
Chl *a* (μg liter^{-1})	X = 8	18–45	8–16	Malone et al. 1986; Shiah and Ducklow 1994; Glibert et al. 1995
PARz$_{0.5}$ (μE m^{-2} s^{-1})	200	299	343	Jones et al. 1990
Bacteria : PC	0.29	0.17–0.21		Estimated from values reported in Malone et al. 1986; Shiah and Ducklow 1994; Glibert et al. 1995

closures of varying dimensions may diverge as the influence of area-to-volume effects on biological components varies. However, the fact that these effects can be consistent may allow investigators to design future mesocosm studies to minimize certain artifacts of enclosure.

References

AXLER, R. P., AND J. E. REUTER. 1996. Nitrate uptake by phytoplankton and periphyton: Whole-lake enrichments and mesocosm-^{15}N experiments in an oligotrophic lake. Limnol. Oceanogr. **41:** 659–671.

BANSE, K. 1992. Grazing, temporal changes of phytoplankton concentrations, and the microbial loop in the open sea, p. 404–440. *In* P. G. Falkowski and A. D. Woodhead [eds.], Primary productivity and biogeochemical cycles in the sea. Plenum.

BJØRNSEN, P. K., B. RIEMANN, S. JESPER HORSTED, T. GISSEL NIELSEN, AND J. POCK-STEN. 1988. Trophic interactions between heterotrophic nanoflagellates and bacterioplankton in manipulated seawater enclosures. Limnol. Oceanogr. **33:** 409–420.

BODE, A., AND Q. DORTCH. 1996. Uptake and regeneration of inorganic nitrogen in coastal waters influenced by the Mississippi River: Spatial and seasonal variation. J. Plank. Res. **18:** 2251–2268.

BRATBAK, G., M. HELDAL, S. NORLAND, AND T. F. THINGSTAD. 1990. Viruses as partners in spring bloom microbial trophodynamics. Appl. Environ. Microbiol. **56:** 1400–1405.

BROCKMANN, U. 1990. Pelagic mesocosms: II. Process studies, p. 81–108. *In* C. M. Lalli [ed.], Enclosed experimental marine ecosystems: A review and recommendations. Springer-Verlag.

CARPENTER, S. R. 1996. Microcosm experiments have limited relevance for community and ecosystem ecology. Ecology **77:** 677–680.

———, S. W. CHISHOLM, C. J. KREBS, D. W. SCHINDLER, AND R. F. WRIGHT. 1995. Ecosystem experiments. Science **269:** 324–327.

CHEN, C.-C., J. E. PETERSEN, AND W. M. KEMP. 1997. Spatial and temporal scaling of periphyton growth on walls of estuarine mesocosms. Mar. Ecol. Prog. Ser. **155:** 1–15.

COALE, K. H., AND OTHERS. 1996. A massive phytoplankton bloom induced by an ecosystem-scale iron fertilization experiment in the Equatorial Pacific Ocean. Nature **383:** 495–501.

COLE, J. J., G. E. LIKENS, AND D. L. STRAYER. 1982. Photosynthetically produced dissolved organic carbon: An important carbon source for planktonic bacteria. Limnol. Oceanogr. **27:** 1080–1090.

CROWDER, M. J., AND D. J. HAND. 1990. Analysis of repeated measures. Chapman and Hall.

DERENBACH, J. B., AND P. J. LE B. WILLIAMS. 1974. Autotrophic and bacterial production: Fractionation of plankton populations by differential filtration of samples from the English Channel. Mar. Biol. **25:** 263–269.

DOERING, P. H., C. A. OVIATT, L. L. BEATTY, V. F. BANZON, R. RICE, S. P. KELLY, B. K. SULLIVAN, AND J. B. FRITHSEN. 1989. Structure and function in a model coastal ecosystem: Silicon, the benthos and eutrophication. Mar. Ecol. Prog. Ser. **52:** 287–299.

EGGE, J. K., AND D. L. AKSNES. 1992. Silicate as regulating nutrient in phytoplankton competition. Mar. Ecol. Prog. Ser. **83:** 281–289.

ELMGREN, R., G. A. VARGO, J. F. GRASSLE, J. P. GRASSLE, D. R. HEINLE, G. LANGLOIS, AND S. L. VARGO. 1980. Trophic interactions in experimental marine ecosystems perturbed by oil, p. 779–800. *In* Microcosms in ecological research, DOE Symposium series 52. Technical information center, U.S. Department of Energy, Washington, D.C.

FRENCH, R. H., AND R. J. WATTS. 1989. Performance of in situ microcosms compared to actual reservoir behavior. J. Environ. Eng. **115:** 835–849.

GLIBERT, P. M. 1998. Interactions of top-down and bottom-up control in planktonic nitrogen cycling, p. 1–12. *In* T. Tamminen and H. Kuosa [eds.], Eutrophication in planktonic ecosystems: Food web dynamics and elemental cycling. V. 363. Hydrobiologia.

———, AND D. G. CAPONE. 1993. Mineralization and assimilation in aquatic, sediment, and wetland systems, p. 243–272. *In* R. Knowles and T. H. Blackburn [eds.], Nitrogen isotope techniques. Academic.

———, D. J. CONLEY, T. R. FISHER, L. W. HARDING, AND T. C. MALONE. 1995. Dynamics of the 1990 winter/spring bloom in Chesapeake Bay. Mar. Ecol. Prog. Ser. **122:** 27–43.

———, C. GARSIDE, J. A. FUHRMAN, AND M. R. ROMAN. 1991. Time-dependent coupling of inorganic and organic nitrogen uptake and regeneration in the plume of the Chesapeake Bay estuary and its regulation by large heterotrophs. Limnol. Oceanogr. **36:** 895–909.

GRASSLE, J. P., AND J. F. GRASSLE. 1984. The utility of studying the effects of pollutants on single species populations in benthos of mesocosms and coastal ecosystems, p. 621–642. Concepts in Marine Pollution Measurements. Technical Report. Maryland University Sea Grant Program.

HEISKANEN, A.-S., T. TAMMINEN, AND K. GUNDERSEN. 1996. Impact of planktonic food web structure on nutrient retention and loss from a late summer pelagic system in the coastal northern Baltic Sea. Mar. Ecol. Prog. Ser. **145:** 195–208.

HOBBIE, J. E., R. J. DALEY, AND S. JASPER. 1977. Use of nuclepore

filters for counting bacteria by fluorescence microscopy. Appl. Environ. Microbiol. **33:** 1225–1228.

JONES, T. W., T. C. MALONE, AND S. PIKE. 1990. Seasonal contrasts in diurnal carbon incorporation by phytoplankton size classes of the coastal plume of Chesapeake Bay. Mar. Ecol. Prog. Ser. **68:** 129–134.

KIRK, J. T. O. 1994. Light and photosynthesis in aquatic ecosystems, 2nd ed. Cambridge Univ. Press.

KROER, N., AND R. B. COFFIN. 1992. Microbial trophic interactions in aquatic microcosms designed for testing genetically engineered microorganisms: A field comparison. Microb. Ecol. **23:** 143–157.

KUIPER, J., U. H. BROCKMANN, H. VAN HET GROENEWOUD, G. HOORNSMAN, AND K. D. HAMMER. 1983. Influences of bag dimensions on the development of enclosed plankton communities during POSER. Mar. Ecol. Prog. Ser. **14:** 9–17.

LALLI, C. M. 1990. Enclosed experimental marine ecosystems: A review and recommendations. Springer.

LANCELOT, C., AND G. BILLEN. 1984. Activity of heterotrophic bacteria and its coupling to primary production during the spring phytoplankton bloom in the Southern Bight of the North Sea. Limnol. Oceanogr. **29:** 721–730.

LANDRY, M. R., AND OTHERS. 1997. Iron and grazing constraints on primary production in the central equatorial Pacific: An EqPac synthesis. Limnol. Oceanogr. **42:** 405–418

LEE, S., AND J. A. FUHRMAN. 1987. Relationships between biovolume and biomass of naturally derived marine bacterioplankton. Appl. Environ. Microbiol. **53:** 1298–1303.

MALONE, T. C., D. J. CONLEY, T. R. FISHER, P. M. GLIBERT, AND L. W. HARDING. 1996. Scales of nutrient-limited phytoplankton productivity in Chesapeake Bay. Estuaries **19:** 371–385.

———, W. M. KEMP, H. W. DUCKLOW, W. R. BOYNTON, J. H. TUTTLE, AND R. B. JONAS. 1986. Lateral variation in the production and fate of phytoplankton in a partially stratified estuary. Mar. Ecol. Prog. Ser. **32:** 149–160.

MCALLISTER, C. D., T. R. PARSONS, K. STEPHENS, AND J. D. H. STRICKLAND. 1961. Measurements of primary production in coastal sea water using a large-volume plastic sphere. Limnol. Oceanogr. **6:** 237–258.

NELSON, N. B., AND B. B. PRÉZELIN. 1990. Chromatic light effects and physiological modeling of absorption properties of *Heterocapsa pygmaea* (=*Glenodinium* sp.). Mar. Prog. Ser. **63:** 37–46.

NIXON, S. W., D. ALONSO, M. E. Q. PILSON, AND B. A. BUCKLEY. 1980. Turbulent mixing in aquatic microcosms, p. 818–849. *In* J. P. Giesy [ed.], Microcosms, ecological research. U.S. Dept. Energy Symposium Series, Augusta, Georgia, 8–19 November 1978, CONF 781101. National Technical Information Service, Springfield, Virginia.

OVIATT, C. A. 1994. Biological considerations in marine enclosure experiments: Challenges and revelations. Oceanography **7:** 45–51.

———, P. LANE, F. FRENCH, AND P. DONAGHAY. 1989. Phytoplankton species and abundance in response to eutrophication in coastal marine mesocosms. J. Plankton Res. **11:** 1223–1244.

———, AND OTHERS. 1987. Fate and effects of sewage sludge in the coastal marine environment: A mesocosm experiment. Mar. Ecol. Prog. Ser. **41:** 187–203.

———, H. WALKER, AND M. E. Q. PILSON. 1980. An exploratory analysis of microcosm and ecosystem behavior using multivariate techniques. Mar. Ecol. Prog. Ser. **2:** 179–191.

PAINTING, S. J., M. I. LUCAS, AND D. G. MUIR. 1989. Fluctuations in heterotrophic bacterial community structure, activity and production in response to development and decay of phytoplankton in a microcosm. Mar. Ecol. Prog. Ser. **53:** 129–141.

PARSONS, T. R., P. J. HARRISON, AND R. WATERS. 1978. An experimental simulation of changes in diatom and flagellate blooms. J. Exp. Mar. Biol. Ecol. **32:** 285–294.

PETERSEN, J. E., C.-C. CHEN, AND W. M. KEMP. 1997. Scaling aquatic production: Experiments under nutrient and light limited conditions. Ecology **78:** 2326–2338.

PILSON, M. E. Q., AND S. W. NIXON. 1980. Marine microcosms in ecological research, p. 724–741. *In* Microcosms in ecological research, DOE Symposium series 52. Technical information center, U.S. Department of Energy, Washington, D.C.

RIEMANN, B., H. M. SØRENSEN, P. K. BJØRNSEN, S. JESPER HORSTED, L. MØLLER JENSEN, T. GISSEL NIELSEN, AND M. SØNDERGAARD. 1990. Carbon budgets of the microbial food web in estuarine enclosures. Mar. Ecol. Prog. Ser. **65:** 159–170.

SANFORD, L. P. 1997. Turbulent mixing in experimental ecosystem studies. Mar. Ecol. Prog. Ser. **161:** 265–293.

SHIAH, F.-K., AND H. W. DUCKLOW. 1994. Temperature regulation of heterotrophic bacterioplankton abundance, production, and specific growth rate in Chesapeake Bay. Limnol. Oceanogr. **39:** 1243–1258.

SIMON, M., B. C. CHO, AND F. AZAM. 1992. Significance of bacterioplankton biomass in lakes and the ocean: Comparison to phytoplankton biomass and biogeochemical implications. Mar. Ecol. Prog. Ser. **86:** 103–110.

SMITH, E. M., AND W. M. KEMP. 1995. Seasonal and regional variations in plankton community production and respiration for Chesapeake Bay. Mar. Ecol. Prog. Ser. **116:** 217–231.

STEPHENSON, G. L., P. HAMILTON, N. K. KAUSHIK, J. B. ROBINSON, AND K. R. SOLOMON. 1984. Spatial distribution of plankton in enclosures of three sizes. Can. J. Fish. Aquat. Sci. **41:** 1048–1054.

TAKAHASHI, M., W. H. THOMAS, D. L. R. SEIBERT, J. BEERS, P. KOELLER, AND T. R. PARSONS. 1975. The replication of biological events in enclosed water columns. Arch. Hydrobiol. **76:** 5–23.

WHITLEDGE, T. E., S. C. MALLOY, C. J. PATTON, AND C. D. WIRICK. 1981. Automated nutrient analyses in seawater. Brookhaven National Laboratories Formal Rep. BNL 51398.

ZIMMERMAN, C., M. PRICE, AND J. MONTGOMERY. 1977. Operation, methods and quality control of Technicon Autoanalyzer II Systems for nutrient determination in seawater. Harbor Branch Foundation, Technical Rep. No. 11.